JOURNAL OF MATERIALS SCIENCE 20 (1985) 2169–2185

Applications of tilted illumination in transmission electron microscopy and diffraction of crystalline materials

J. R. WHITE,* E. L. THOMAS
Department of Polymer Science and Engineering, University of Massachusetts, Amherst, Massachusetts 01003, USA

Diffraction contrast depends on the relative orientation of the electron beam and the crystals in a polycrystalline sample. Tilting the illumination will therefore alter image contrast, and the consequences of changing the illumination direction rather than the specimen attitude (using a goniometer) are examined. The electromagnetic tilt controls permit very accurate tilts to be set up very easily and quickly, a feature of special importance when dealing with radiation-sensitive crystals. The effect on both dark- and bright-field imaging is considered. The loss of resolution that happens when the beam is tilted does not seriously detract from the overall image quality when operating at low magnification, as is often the case with beam-sensitive specimens. Examples of tilted-beam operation are presented for polycrystalline gold and polyethylene samples.

1. Introduction

Most transmission electron microscopes are provided with a set of electromagnetic coils in the illumination system for tilting the electron beam. The primary reason for including this device is to permit tilted-illumination dark-field operation. In this mode it is arranged that the diffracted beam to be used to form the dark-field image passes along the optic axis of the objective lens, so minimizing spherical aberration. The appropriate illumination tilt is (minus) $2\theta_{hkl}$ where θ_{hkl} is the Bragg angle for the chosen beam, and the microscope is adjusted while viewing the selected-area diffraction pattern. The normal procedure is to note the position of the undeflected illumination (the central transmitted beam) then to bring the chosen diffracted beam to this position using the tilt coils [1, 2]. A similar procedure can be employed when forming high-resolution images using two or more beams (which might include the transmitted beam) for imaging. In this case best resolution is obtained when the beams are symmetrically distributed about the optic axis, so that the same spherical aberration phase-shift is suffered by each beam [2–4]. For such operation the tilt adjustment is again made with reference to the diffraction pattern, using the objective aperture to mark the position of the objective optic axis, but in this case the objective aperture must be of quite critical dimensions and rather larger than is normally employed in single-beam dark-field operation as described here.

The purpose of the current paper is to describe the consequence of using tilted illumination with crystalline specimens. Particular attention is given to the use of tilts other than $2\theta_{hkl}$, to the effect of beam tilt on bright-field images, and to the combined effect of beam tilt and defocus. The procedures described here were developed initially for use with polycrystalline polymer specimens, but some of the results presented below were obtained with evaporated gold specimens which are simple to make, and which do not suffer from the problem of rapid deterioration in the electron beam.

Permanent address: Department of Metallurgy and Engineering Materials, University of Newcastle-Upon-Tyne, UK.

0022–2461/85 $03.00 + .12

2. Specimen preparation

2.1. Thin gold films

Gold films were prepared by evaporating 0.2 mm diameter wire using a tungsten filament. The film thickness was estimated from the length of wire and the distance between the source and the (glass) substrate by assuming spherically symmetric distribution; the value was ~ 30 nm. The as-evaporated grain size is rather small when using a cold (room-temperature) substrate, and some films were heated in an air oven at 170° C while still on the substrate to promote grain growth [5]. The films were scored, floated on to water and picked up on electron microscope grids.

Films of much smaller average thickness are discontinuous, and were produced by evaporating on to evaporated carbon films which were already mounted on electron microscope grids.

2.2. Oriented polyethylene film

Some of the experiments described here were conducted on melt-drawn high-density polyethylene films prepared by D. C. Yang using the method introduced by Petermann [6, 7] and further developed by Yang and Thomas [8]. A solution of polyethylene in xylene (~ 0.5 wt %) was cast on to a pre-heated glass plate (120 to 125° C) and the solvent allowed to evaporate. A thin film (50 to 100 nm thick) was then drawn off at a constant rate (~ 40 mm min^{-1}). Films were inspected both in the as-drawn state and after annealing at temperatures in the range 120 to 130° C. Detailed discussion of the structure of these films has been presented elsewhere [8].

3. Modes of operation of the electron microscope

In this section we will describe several modes of operation of the conventional transmission electron microscope (TEM) in which tilted illumination may be exploited to advantage. The first technique is the well-known tilted dark-field method, which is included here as a convenient introduction to the less conventional procedures described later.

3.1. Tilted dark-field

In the tilted dark-field technique the first step is to obtain a selected-area diffraction pattern with the tilt coils unexcited. The central beam defines the optic axis of the objective lens if the instrument has been properly aligned, and its position on the viewing screen must be marked; this may be achieved using the beam stop if its shadow is sufficiently small, or by centring an objective aperture around the main beam. The chosen diffraction beam is then brought to this position by activating the tilt coils, the effect of which is to shift the diffraction pattern on the viewing screen. In this state the diffracted beam passes along the optic axis of the objective lens and, with the objective aperture centred about this direction, this becomes the image-forming beam when the microscope is returned to imaging conditions. This arrangement minimizes spherical aberration, and for this reason this technique is often referred to as "high resolution dark-field" [1].

Schematic diagrams of the electron ray paths are shown in Fig. 1. Fig. 1a depicts untilted illumination, and the undeviated or transmitted beam T appears at the centre of the diffraction pattern obtained by imaging the back focal plane of the objective lens. The objective aperture is located in this plane and is centred around T for bright-field diffraction contrast imaging. A diffracted beam is shown at D, and dark-field conditions using this beam can be obtained simply by shifting the aperture across to this position, permitting only those electrons which have suffered this particular deflection to form the image ("shifted aperture dark-field" imaging). Since these electrons are inclined to the optic axis, this method introduces significant spherical aberration. The alternative of tilted dark-field operation is shown in Fig. 1, which shows the same pair of beams T and D. This time D is at the position formerly occupied by T when using untilted illumination. In most modern TEMs at least two circuits are provided for energizing the tilt coils. These can be pre-set independently for bright-field and for dark-field from a particular beam respectively (or for dark-field from two different selected beams), and the change from one to the other is achieved at the throw of a switch.

Although tilted dark-field is preferred if resolution must be maximized, there are other considerations. When using the tilted dark-field method the illumination makes a different angle to the diffracting planes for bright-field and dark-field imaging respectively. For a typical layer-plane spacing (say 0.4 nm) and for 100 keV electron energy (giving an electron wavelength of

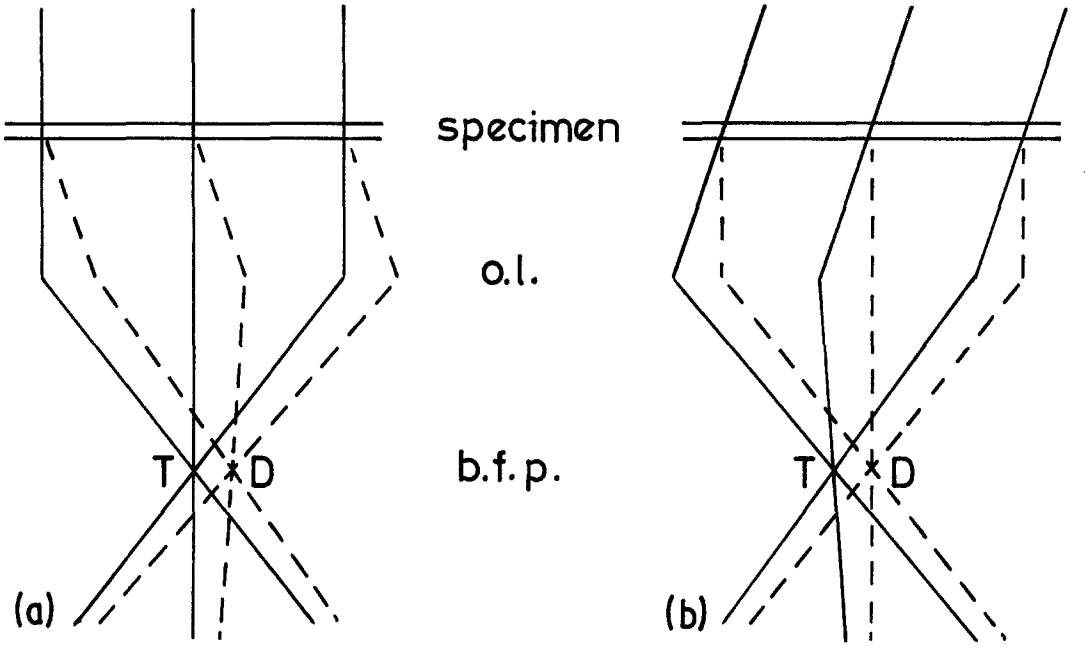

Figure 1 Electron paths through the specimen, objective lens (o.l.) and back focal plane (b.f.p.). Solid lines: transmitted electrons (T); broken lines: diffracted electrons (D). (a) Transmitted beam parallel to optic axis, (b) tilted illumination.

0.0037 nm) the required tilt amounts to ~ 10 mrad (~ 0.5°). To assess how significant this might be it is useful to consider the rocking curve for a thin crystal. This defines the rate at which diffracted intensity falls off as the crystal is rotated away from the exact Bragg orientation. For a thin crystal of low atomic number for which kinematical conditions hold [5], this curve is given by $(\sin^2 \pi st)/(\pi s)^2$, where s defines the misorientation from the Bragg position (Fig. 2) and t is the crystal thickness, measured along the illumination direction assuming negligible beam divergence [1, 9].

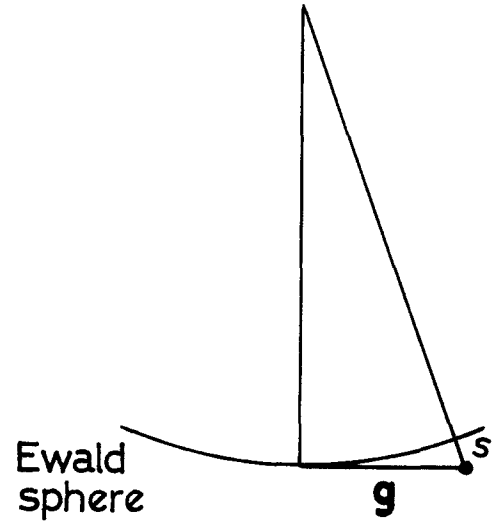

Figure 2 Ewald sphere construction, defining misorientation parameter s for the diffracted beam corresponding to the reciprocal lattice vector g.

If the subsidiary maxima of the above function can be ignored, then the maximum misorientation from the Bragg position for which observable intensity can be obtained can be taken to be slightly inside the positions of the first zeros of the function, i.e. $s = \pm 1/t$. Thus the limiting misorientation ω from the Bragg position is approximately $\pm 1/gt = \pm d_{hkl}/t$ where g is the magnitude of the reciprocal lattice vector (Fig. 2). For $d_{hkl} = 0.4$ nm and $t = 10$ nm this becomes ± 0.04 rad. The Bragg angle is clearly significant when compared with this value and becomes increasingly significant as the crystal thickness increases, so the illumination tilt angle will have a strong influence on the diffracted intensity when using high resolution dark-field conditions. This must be kept in mind when comparing bright-field and dark-field images from the same area, especially if an attempt is made to assess the extent to which they are complementary.

One further point to note is that in the symmetrical position, in which the electron beam is exactly parallel to the zone axis corresponding to

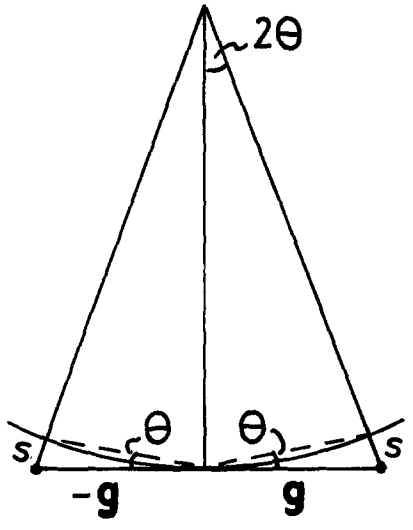

Figure 3 Ewald sphere construction for a crystal in the symmetrical position for planes with reciprocal lattice vectors g and $-g$.

the section of the reciprocal lattice sampled by the Ewald sphere, the misorientation from the Bragg position for both reflections (hkl) and $(\bar{h}\bar{k}\bar{l})$ (corresponding to g and $-g$ respectively in Fig. 3) will be of magnitude θ_{hkl}. Hence for a crystal of thickness greater than $2d^2/\lambda$ no diffraction should be seen, provided that kinematical conditions pertain, beam divergence is much less than θ_B (the Bragg angle) and the crystal is not bent. These conditions are extremely unlikely to be fulfilled.

3.2. Hybrid dark-field operation

3.2.1. Setting the tilt

Up to now only two types of dark-field operation have been considered:

(a) high-resolution dark-field in which the diffracted beam is moved by tilting the illumination so that it passes through the objective aperture (which remains undisplaced from the optic axis of the objective lens) and

(b) shifted-aperture dark-field in which the illumination remains parallel to the optic axis of the objective lens and the objective aperture is moved across to admit the diffracted beam.

We will now consider a hybrid method in which the beam is tilted by an amount other than $2\theta_{hkl}$ (greater or smaller and possibly about a different axis) so that it is also necessary to shift the objective aperture in order to allow the selected beam to pass through. Here the purpose of tilting the illumination is not to permit high-resolution operation, but to change the diffraction condition. The same could be achieved by tilting the specimen using a goniometer stage. The reasons for recommending the beam-tilt option, and the circumstances in which it can be of particular advantage, will now be discussed.

In setting a particular illumination tilt the selected-area diffraction pattern is first obtained. The direction of beam tilt required will be specified in terms of the crystal orientation, which is revealed by the diffraction pattern. On tilting the illumination the pattern will shift, and the direction and magnitude of the shift will accurately specify the direction and magnitude of the tilt obtained by changing the excitation of the tilt coils. If a measured tilt is required in a particular direction, the adjustment can be made by repeatedly switching between the bright-field setting (in which the illumination tilt coils retain the setting obtained during a preliminary accurate alignment of the microscope, leaving this as a reference state) and the dark-field setting, for which the tilt coils are altered to give a shift in the required direction and of the correct magnitude. The magnitude of the tilt can be judged with reference to the diffraction pattern, which acts as a calibrant for the tilt.

The best method of measuring the tilt is to double-expose a diffraction pattern firstly with bright-field setting, and then with dark-field setting (Fig. 4). It is recommended that the filament current is switched off before changing from bright-field to dark-field during the exposure; the beam may otherwise shift momentarily to different positions while changing from one condition to the other, and an artefact may be recorded on the photograph. The reflections belonging to the respective patterns obtained with different illumination directions can be readily distinguished, and the shift (which will be the same for each reflection and equal to the shift of the transmitted beam) can be measured quite accurately from the plate by using any (or many) suitable reflections. If a very low exposure is used the transmitted beam may be suitable for this measurement, but more often this beam will be broadened both by inelastic scattering, which is significant in directions close to the beam, and as a consequence of overexposure. The diffraction spots or rings will usually be sharper, and hence more suitable for the shift measurement. We estimate that the tilt can be measured to better

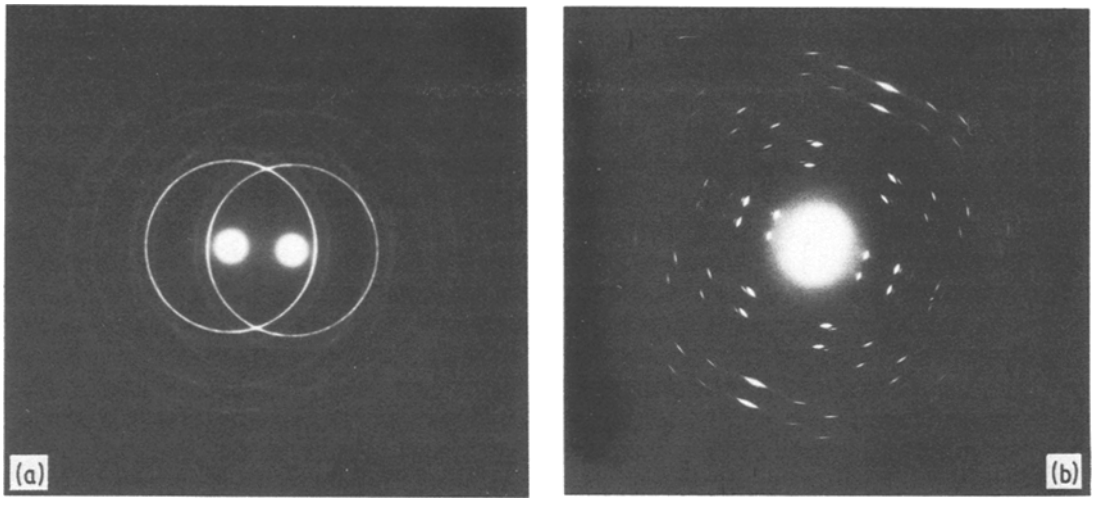

Figure 4 Double-exposure electron diffraction patterns with a relative shift produced by tilting the illumination between exposures. (a) Polycrystalline gold, (b) oriented polycrystalline polyethylene.

than ± 0.01° with this method, though the accuracy will vary with the sharpness of the pattern.

As described above, the direction of tilt is fairly easily set, especially if the corresponding shift is parallel to one of the prominent reciprocal lattice vectors displayed in the diffraction pattern. The exact magnitude is not known until subsequent measurement from the double-exposure diffraction pattern, but it would not be difficult to measure the shift during electron-optical operation by providing an eyepiece measuring device (e.g. a graticule or micrometer-driven crosswire) in the binoculars used for viewing the screen. Alternatively, the currents in the tilt coils could be monitored and calibrated; reasonable accuracy has been claimed for this approach [10–12].

After setting the tilt, the objective aperture drives are used to centre the aperture about the beam to be used for dark-field imaging and the instrument is returned to imaging conditions.

3.2.2. Comparison of tilted-illumination with tilted-specimen operation

As already stated, a change in diffraction condition can be achieved either by tilting the illumination or by tilting the specimen. The tilted-illumination technique, as described above, is very simple and quick to arrange; it contains its own calibration when working with crystalline specimens of known spacings, and is capable of high accuracy within the limited tilt magnitude available. Beam tilts of ± 5° and more can be obtained easily, but significant image deterioration occurs when working near the limits of this range where coma [13, 14] is a serious problem. The alternative of tilting the specimen requires the use of a double-tilt goniometer, except when tilts are required about one axis only and the specimen has known orientation permitting insertion into a single-tilt holder in the appropriate orientation. The setting of a chosen tilt when the specimen is mounted in an arbitrary orientation in a double-tilt goniometer is possible, but not a simple procedure. The precision with which tilts can be set in an electron microscope is not very high for many goniometers in popular use, and ± 1° is quite normal. Thus accurate work within the range say −3° to +3° is often out of the question, and settings less than 0.5° apart almost impossible to achieve. Finally, when tilts are obtained using a goniometer, differences in focus will be obtained over the field of view. These may be significant even at small tilts (< 3°) and will usually constitute a disadvantage. Thus, the use of tilted illumination is for many purposes the preferred method for setting up a modified diffraction condition, unless a high-resolution requirement demands that the diffracted beam used for imaging must pass along the optic axis of the objective lens.

For large tilts there is no alternative to using the goniometer, but the final tuning can still be made easier by the use of the tilted-illumination method. It is worth noting here that goniometers are now available that are capable of much higher accuracy, and that highly accurate settings are

possible in favoured circumstances. There are many examples in the literature of the use of Kikuchi lines [2] to determine crystal orientation, and it has been shown that they can be used to set a pre-determined orientation using a goniometer. Such an approach can only be utilized with fairly thick specimens, for Kikuchi lines are a dynamical phenomenon. It is essential also that specimens do not suffer damage in the electron beam, for extended observation is necessary while making the required adjustments. It must therefore be emphasized that the principal value of the electromagnetic beam-tilt procedure will be found where specimens have small mass thickness and are beam-sensitive, demanding rapid selection and adjustment of imaging conditions.

In a later section we will give examples of the kind of study in which a small relative tilt between the illumination and the specimen provides valuable structural or morphological information. For the present it is sufficient to take an extreme example by noting that a crystal which is Bragg-oriented, and thus appears bright in the original (untilted) dark-field condition, will no longer diffract if the illumination is tilted sufficiently, and will be dark in dark-field conditions after applying the tilt.

3.3. Tilted-illumination bright-field operation

Just as tilting the illumination to alter the diffraction conditions will modify contrast in dark-field operation, so will contrast be modified if the image is formed with the transmitted beam. Taking the same example as above, a crystal which in its original imaging condition was diffracting strongly will appear dark under bright-field imaging, but when the illumination is tilted so that Bragg's law is no longer fulfilled, less intensity will be lost from the transmitted beam and the crystal will appear brighter in bright-field conditions.

To arrange for tilted-illumination bright-field imaging conditions the tilt is set up exactly as described in Section 3.2, and the objective aperture is then centred about the central transmitted beam in the diffraction pattern. This will, of course, mean displacing it from the optic axis of the objective lens, giving rise to shifted-aperture bright-field conditions. Although this might seem to be a roundabout way of adjusting the instrument for poorer-than-optimum resolution in bright-field, the benefits from this procedure are similar to those listed for the equivalent dark-field technique; that is, modified diffraction conditions can be set rapidly and accurately and give rise to contrast changes which provide structural and morphological information not readily obtained by other methods.

4. Properties of tilted-illumination diffraction patterns and images

4.1. Calibration of the tilt

Consider the diffraction pattern formed with untilted illumination. For camera length L the displacement of a beam deflected at an angle β from the transmitted beam will be $L \tan\beta$ (Fig. 5). For all but the most accurate work the small-angle approximation is valid, and this displacement becomes $L\beta$. For a Bragg-diffracted beam $\beta = 2\theta_{hkl}$. Thus the angle of tilt from the transmitted beam of an observed (e.g. diffracted) beam is linearly related to its measured separation from the position of the transmitted beam in the diffraction pattern, and any diffraction spot from planes of known spacing can be used to calibrate the pattern. Similarly, if the illumination is tilted through an angle α the transmitted beam

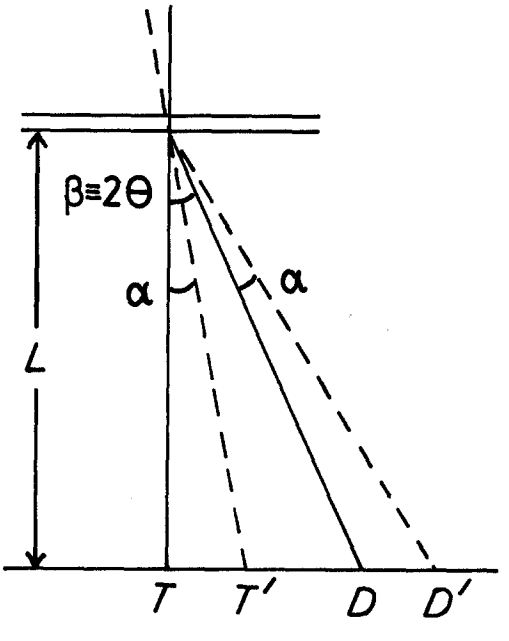

Figure 5 Schematic diagram of diffraction geometry for untilted illumination, giving rise to a transmitted beam at T and a diffracted beam at D (solid lines) and for tilted illumination, giving rise to a transmitted beam at T' and a diffracted beam at D' (broken lines).

will be displaced by a distance $L\alpha$ from the position in the untilted condition. To measure the displacement the double-exposure method described above is preferred, since successive plates or films will not locate accurately at the same position in the microscope camera. Thus, if the spacing d_{hkl} of the (hkl) planes is known, and if the corresponding reflection appears at a distance r_{hkl} from the centre of the diffraction pattern, then $L = r_{hkl}/2\theta_{hkl}$.

Hence, if tilting the illumination gives a displacement x on the same pattern the magnitude of tilt will be $x\lambda/r_{hkl}d_{hkl}$ where λ is the wavelength. For example, if the polyethylene (0 0 2) reflection is selected for calibration purposes $d_{hkl} \equiv d_{002}$ is 0.254 nm, and measurements taken from Fig. 4b give the ratio $x/r_{hkl} = 0.068$. The electron wavelength for 100 keV electrons, as used to obtain Fig. 4b, is 0.0037 nm so the tilt angle is equal to 0.002 radians or 0.114°.

4.2. Effect of tilt on defocused images

There are several sources of contrast in the electron image, and the instrument is normally adjusted to give conditions in which one of these is dominant. This normally simplifies the resultant image and aids interpretation. Phase contrast is important in many applications, ranging from lattice imaging to the observation of phase-separated non-crystalline polymers. Phase contrast is very sensitive to defocus, and the optimal defocus depends on the spatial frequency of the features under scrutiny. Large spatial frequencies require a large amount of defocus, and this may lead to a reduction in resolution.

In the study of polycrystalline materials it has been found when using phase-contrast conditions, with no objective aperture in place, that diffraction-related contrast is present. A crystal in a diffracting orientation appears rather darker than surrounding crystals, and in addition a bright "ghost" image can often be found [9]. This ghost image is formed by the diffracted electrons, and is displaced from the bright-field image by an amount which depends on the defocus and in a direction perpendicular to the corresponding diffracting planes. An image formed under these conditions thus contains crystallographic information, for the exact orientation of a diffracting crystal can be determined if the magnitude and direction of the ghost displacement are measured. Alternatively, the magnitude of ghost displacement can be used to calibrate the amount of objective-lens defocus.

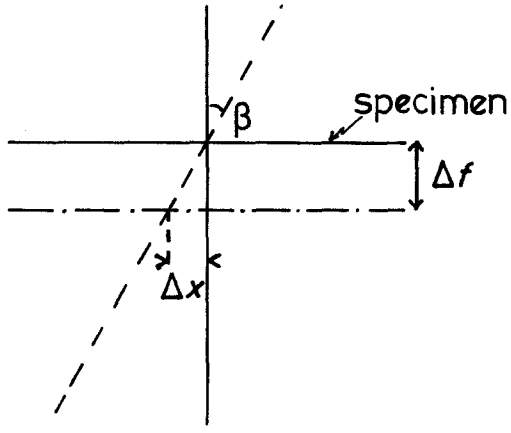

Figure 6 The effect of tilting the illumination (broken line) when the objective lens is defocused an amount Δf. The image of the point at which the electron beam impinges on the specimen shifts by an amount $\Delta x = \beta\Delta f$ when the illumination is tilted through an angle β.

If the electron beam is now tilted, different crystals will be made to diffract and the analysis can be extended. It must be realized, however, that the interaction of tilted illumination and a defocused objective lens causes the image to shift. The reason for this is indicated in Fig. 6, and it can be seen that the image shift will be $\beta\Delta f$ in the direction of tilt where β is the tilt magnitude and Δf is the defocus. There is an addition (though usually negligible except when $\Delta f \sim 0$) a shift $C_s\beta^3$ which depends on the spherical aberration coefficient C_s. This phenomenon is exploited in the procedure often recommended for the alignment of the illumination. In many TEMs a high-voltage "wobbler" is provided which superimposes a varying field on to the accelerating potential. This has the same effect as cyclically varying the strength of the objective lens, and if the illumination is not parallel to the optic axis of the objective lens then the image shifts backwards and forwards across the screen in synchrony with the high-voltage pulsation. The illumination tilt controls can be adjusted to eliminate this motion, and this provides a convenient way of aligning the illumination with the objective lens with high accuracy.

5. Applications and results

We first employed beam tilt to promote modified contrast conditions during studies of polymer

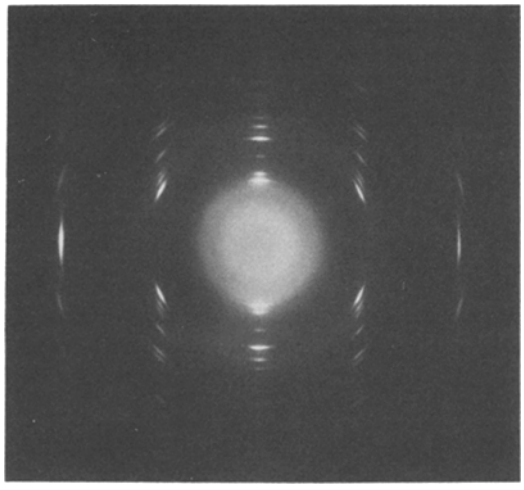

Figure 7 Electron diffraction pattern from oriented polycrystalline polyethylene. For indexing see [8].

samples. The results of these studies will be presented elsewhere, and will be discussed mainly from a materials standpoint rather than emphasizing the techniques used to obtain the structural information. We present here some extracts from these studies together with results obtained with specimens prepared solely for the purpose of testing the procedure described here. All the electron microscopy presented here was conducted on a JEOL 100 CX TEM equipped with a side-entry goniometer and operated at 100 keV. Careful alignment and good beam coherence are important in studies of the kind described here, even when working at low magnifications and low resolution. It is especially important to balance the upper and lower dark-field tilt coils, using the appropriate wobbler circuit provided. Electron micrographs of beam-sensitive polymers were recorded on fast X-ray sensitive film, either Dupont Cronex or Kodak DEF–5.

5.1. Dark-field operation with a polycrystalline sample

A typical diffraction pattern from drawn solution-cast polyethylene film (made as outlined in Section 2.2) is shown in Fig. 7. The crystals are arranged in lamellae with the *c*-axis (molecular axis) parallel to the draw direction and to the lamellar normal. A detailed description of the structure of these films has been presented previously [8]. Only a fraction of the crystalline material is diffracting into the ($h\,k\,0$) reflections at any set condition, and it is concluded that the crystals are either very small, measuring tens of nanometres along the lamellae, or they must contain sufficient distortion to permit parts to be diffracting strongly while neighbouring parts hardly diffract at all. Dark-field images using the combined (1 1 0) and (2 0 0) reflections are shown in Fig. 8; the same area is shown imaged using high-resolution (tilted-beam) dark-field conditions, and using shifted-aperture (untilted) dark-field conditions.

Many crystals are visible in both images, but careful comparison reveals that there are also many examples of crystals which are strongly diffracting in one of the images but hardly

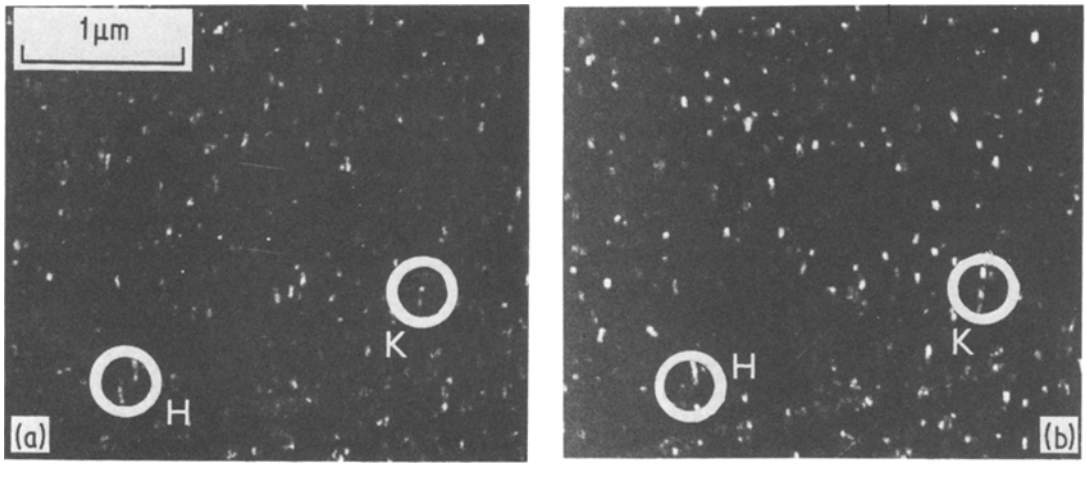

Figure 8 (a) High-resolution dark-field image of oriented polycrystalline polyethylene using the (1 1 0) and (2 0 0) reflections combined. (b) Simple dark-field image (shifted-aperture conditions) of same area using the (1 1 0) and (2 0 0) reflections. Some crystals diffract strongly in both (a) and (b), some in one but not in the other. Examples of both kinds can be found within the areas marked H and K.

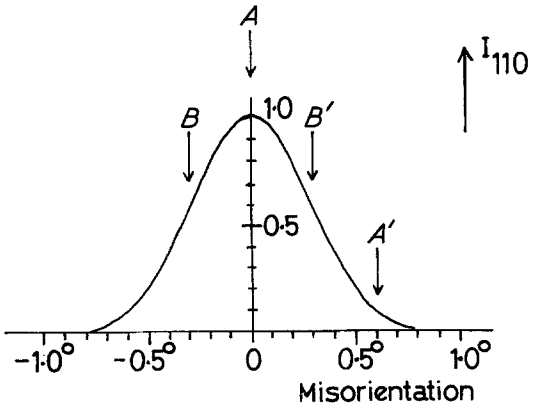

Figure 9 Rocking curve for a polyethylene crystal 30 nm thick for 100 keV electrons.

diffracting at all in the other. The reason for this is, of course, that tilting the beam by the amount required to establish high-resolution dark-field conditions, in this case ~ 0.01 rad or 0.6°, is sometimes sufficient to violate the Bragg condition. This is best understood by reference to the rocking curve (Fig. 9). The rocking curve has been constructed for a polyethylene crystal 30 nm thick, and for the (1 1 0) reflection and 100 kV accelerating potential [9]. The curve shows the intensity obtained both for positive and negative misorientations from the Bragg position. For a crystal which is exactly in the Bragg orientation for untilted illumination the "shifted-aperture" dark-field image will have maximum brightness (as at Position A in Fig. 9). Tilting through 0.6° will cause the intensity to drop to a very low value (as at A'). On the other hand if a crystal is initially slightly misoriented from the Bragg position with untilted illumination the intensity may be significant (B in Fig. 9), and may still remain significant after tilting through 0.6° in the appropriate sense (B' in Fig. 9).

Although these polyethylene films are convenient to illustrate certain image-contrast features as a consequence of their special structure, they are difficult to work with because of their electron-beam sensitivity. Some further detailed dark-field experiments were therefore carried out on gold films. The polycrystalline gold diffraction pattern is a typical face-centred cubic powder-sample ring pattern. To obtain dark-field, part of the diffracted intensity must be sampled, and in Fig. 10 the images were formed by part of the (1 1 1) and (2 0 0) rings. These rings are quite close together, and it is not easy to select one or the other exclusively with apertures within the size range normally provided in a TEM; there is a further problem with many microscopes in that the objective aperture is not located exactly in the

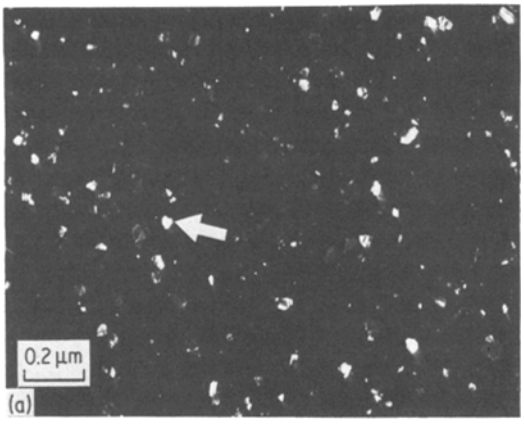

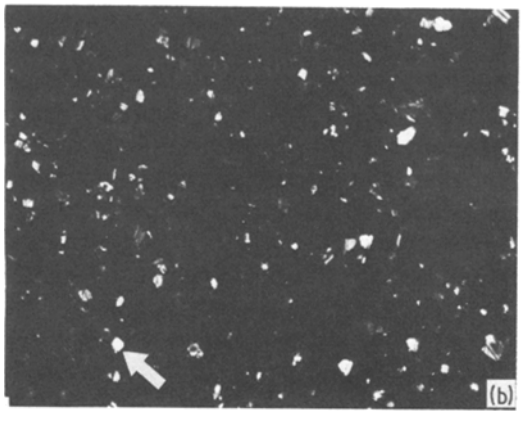

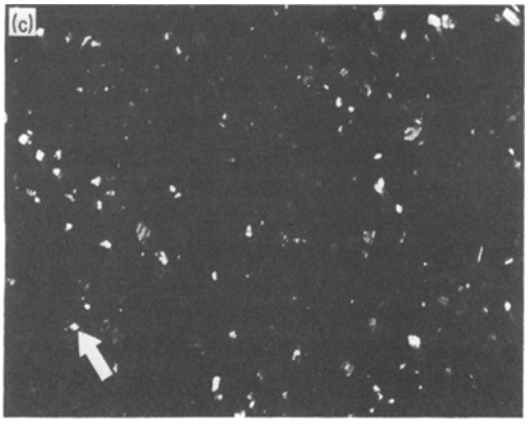

Figure 10 Dark-field micrographs of polycrystalline gold using part of the (1 1 1) and (2 0 0) rings. (a), (b) and (c) show the same area using different illumination tilts. In each photograph an arrow indicates an example of a crystal which is diffracting strongly, but which diffracts only weakly in the other two photographs.

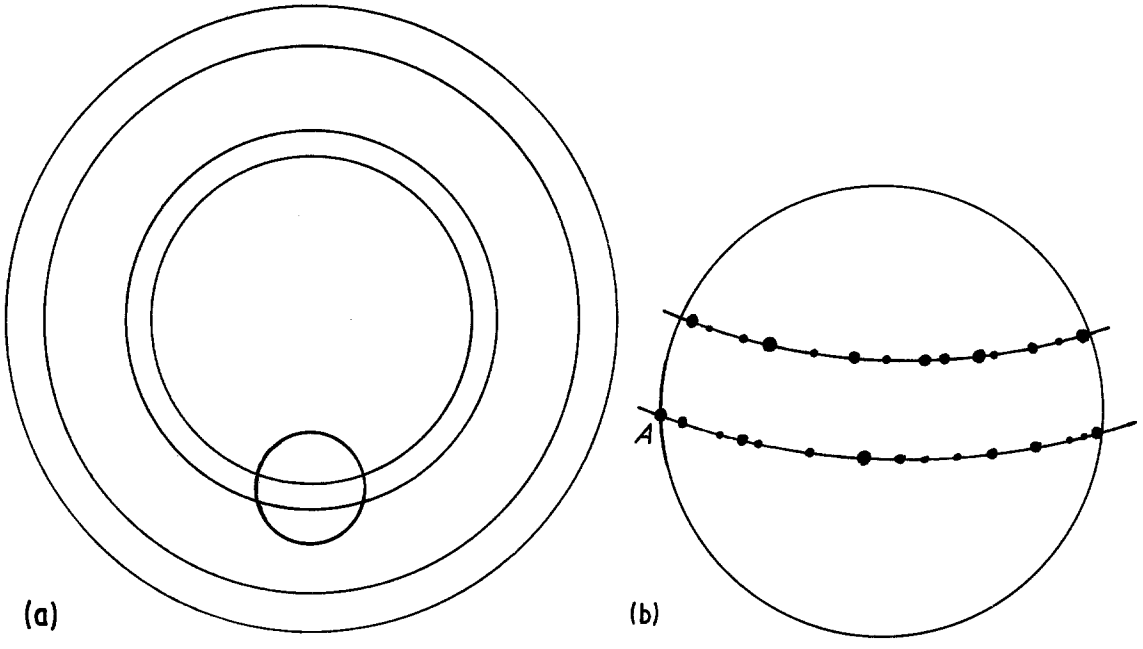

Figure 11 (a) Schematic diagram of an electron-diffraction ring pattern for a polycrystalline specimen, with diameters approximately coincident with the first four rings in a face-centred cubic pattern. The small circle represents the image of an objective aperture set for dark field imaging. (b) Detail within the aperture image at higher magnification at which individual diffraction spots, each belonging to a particular crystal, become distinguishable.

back focal plane of the objective lens, making accurate selection of the scattering range even more difficult to achieve.

In obtaining dark-field images at different tilts it is important to include the same part of the diffraction ring each time if the effect on the appearance of a particular crystal is required. It is fairly easy to set the objective aperture at the correct radial position each time, but the azimuthal adjustment is more difficult for a ring pattern, yet just as critical. This can be seen on reference to Fig. 11, in which the position of the objective aperture is shown in relation to the diffraction pattern. The rings are composed of fine diffraction spots, each produced by a particular crystal. If the position of the aperture is such that the spot at A is just included for one image but just excluded for another, the crystal giving rise to this spot will appear in the first image but not in the second; the interpretation of its "disappearance" will be ambiguous, for this would also be the result if tilting the illumination caused the crystal to stop diffracting.

To minimize the chance of "losing" a crystal because of inaccurate location of the objective aperture in a series of pictures taken with different tilts (Fig. 10) the following procedure was used. The direction of travel of the objective aperture with respect to the diffraction pattern was determined by using one of the aperture-drive controls only, and all electromagnetic tilts were made in the same direction. Each time a new tilt was applied, it was ensured that the central spot could be made to fall centrally within the objective aperture by shifting the aperture using only the chosen drive. In this way the same parts of the (1 1 1) and (2 0 0) rings were selected on using the same control to shift the aperture to the appropriate radius. Naturally a reflection located exactly at the aperture boundary, as at A in Fig. 11, will always present a problem, but if a particular feature is being observed a check can be made by giving the aperture a small tangential displacement in both directions with the second drive control; a crystal which disappears because its diffracted beam is excluded from the aperture will suddenly reappear, whereas changing the position of the aperture in this way will make no difference to the intensity with crystals which are simply not in a diffracting orientation. In the example shown in Fig. 10 it was noted that, within the narrow range of tilts employed, most crystals diffracting significantly in one of the tilt conditions used give at least

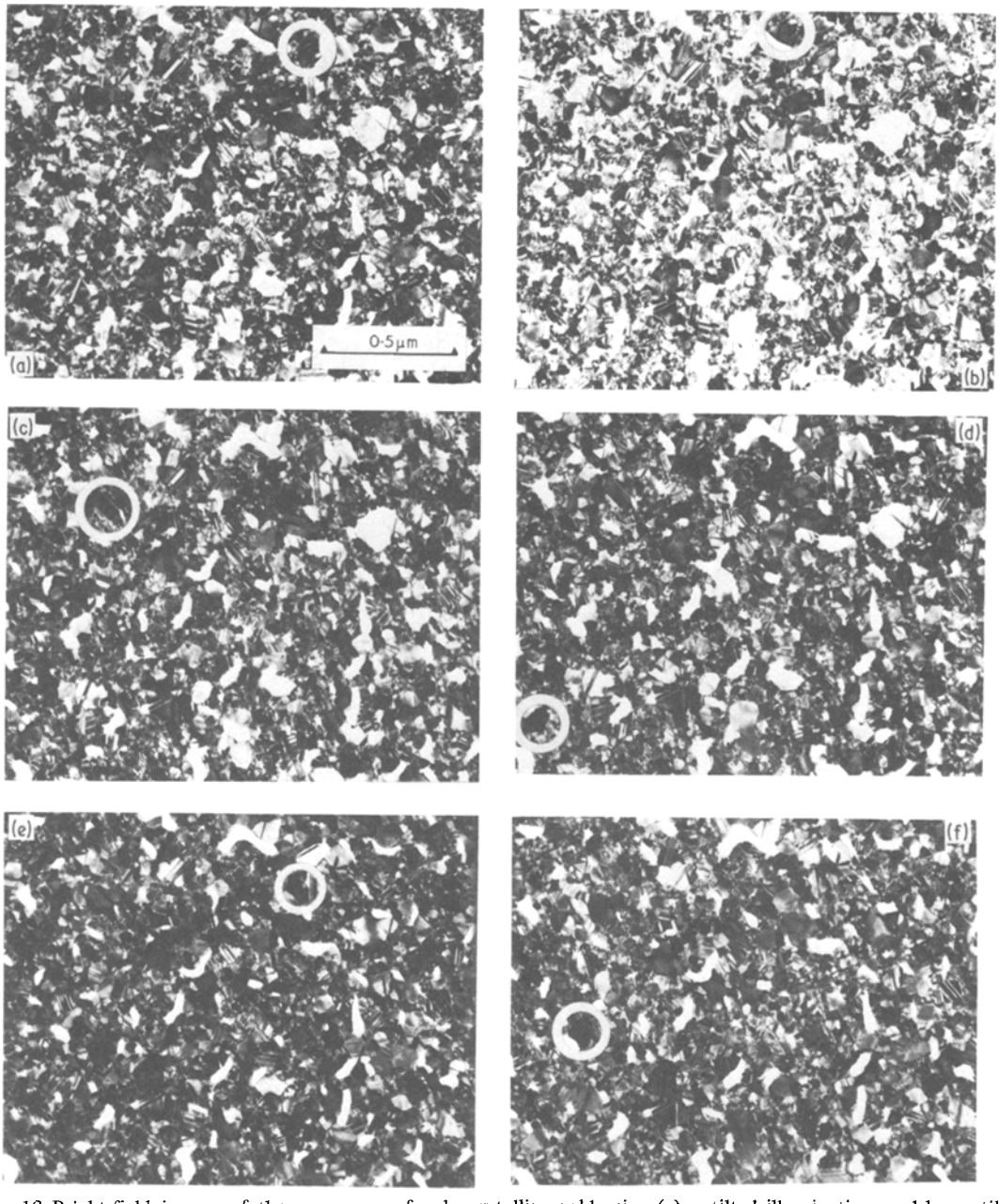

Figure 12 Bright-field images of the same area of polycrystalline gold using (a) untilted illumination, and beam tilts of (b) 0.22°; (c) 0.69°; (d) 1.01°; (e) −0.34° and (f) −0.92°. All tilts were about the same axis, and those used for (e) and (f) were in the opposite sense to those used for (b), (c) and (d). In each photograph a crystal which diffracts much more strongly than under the other imaging conditions has been circled.

a residual image of very low intensity for the other tilts. This showed that the diffraction spot had not been excluded, but was present at an intensity significantly lowered as a consequence of the deviation from the diffracting condition.

Figs. 10a to c show the same area, imaged using the same part of the (1 1 1) and (2 0 0) diffraction rings and using different illumination tilts. In each case a crystal has been indicated which diffracts strongly only in the picture in which it is marked, but which is present only at very low intensity in the others. This indicates the sensitivity of even small crystals (for which the Laue conditions are somewhat relaxed) to beam tilt.

5.2. Bright-field imaging

Fig. 12 shows a series of images taken from the same area in a sample of polycrystalline gold, using shifted-aperture bright-field conditions and various illumination tilts. There are many detailed differences between any chosen pair, but for illustration one crystal only has been circled in each picture. A different crystal is indicated in each picture, and it can be seen that the crystal chosen diffracts strongly (producing a dark image in bright-field) only under the condition used for the picture in which it is marked. As well as differences in intensity shown by individual crystals under different illumination tilts, it can also be seen that there are significant differences in detail within some of the grains.

When evaporated onto an amorphous substrate held at room temperature, gold forms very small crystals and even at a modest annealing temperature (e.g. 170° C as used here) significant grain growth is promoted. Hence most of the grains shown in Figs. 10 and 12 were formed from more than one nucleus, and there remain in some of them sharp crystallographic boundaries separating regions of different crystal orientation (which are often twins). These appear with high contrast when using appropriate diffraction-contrast conditions, but comparison of the photographs shown in Fig. 12 shows that they can be made to disappear by changing the imaging conditions slightly. The interpretation of such features is beyond the scope of this paper, but it does indicate that small amounts of tilt can provide information which may help to probe the structure of the material under inspection.

5.3. Defocused image shift with tilted illumination

Fig. 13 illustrates image shift obtained on tilting the illumination when the objective lens is defocused. The specimen is a polycrystalline gold film. A double exposure has been taken with the illumination beam in the untilted and tilted settings. The amount of tilt applied can be measured using a double-exposure diffraction pattern. The image shift is easily measured on the double-exposure micrograph, and should be proportional to the product of defocus and tilt. A hole or edge can be used for this purpose, but the image of a grid bar should not be used because its shadow will be displaced on tilting the illumination (even in the focused image) because of its significant depth, and the need to separate this effect from the one arising from defocus adds an unnecessary complication.

A single-exposure micrograph of the same area should be recorded because features are often difficult to distinguish in the overlap region. Separation of the two superimposed images and the consequent shift measurement is often easiest to achieve using the negative of the double exposure plus a single-exposure negative. (Single-exposure micrographs of the area shown in Fig. 13 are presented later in Fig. 16.)

Another feature of interest in defocused bright-field studies is the dark-field ghost image of a crystal which is visible when using a large objective aperture, or when operating with the objective aperture withdrawn altogether. When using large values of defocus the bright-field image of a small crystal and its dark-field ghost(s) become

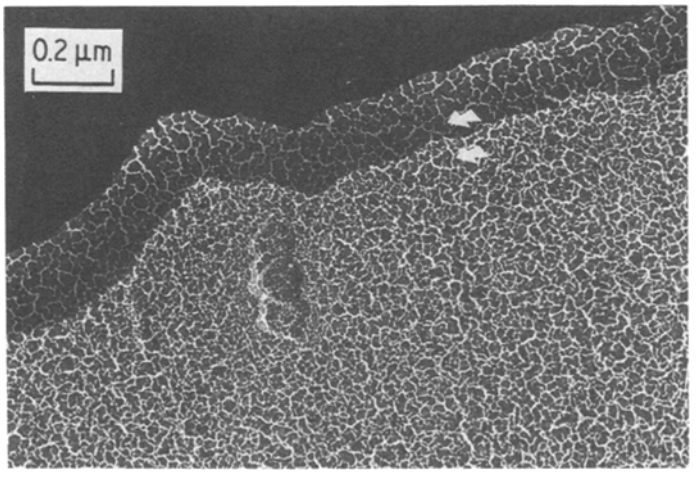

Figure 13 Underfocused images of polycrystalline gold film taken with no objective aperture, using untilted illumination and illumination tilted through 0.66° for a double exposure. The edge of a grid bar crosses the field of view, but should not be used to assess image shift; features recognizable in both images should be used for this purpose, see for example the crystal indicated by the arrows.

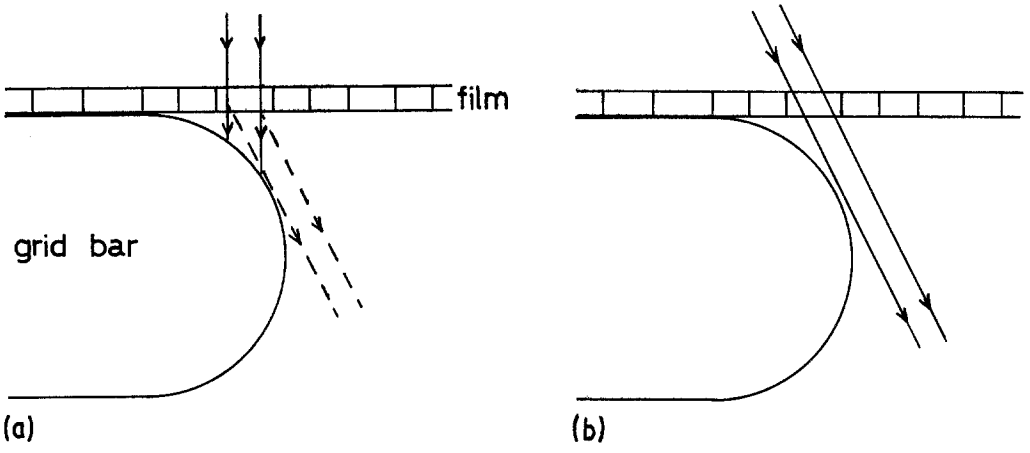

Figure 14 Thin polycrystalline film supported on an electron microscope grid. (a) Untilted illumination. A crystal near to the edge of the grid bar is shown illuminated by the beam. The transmitted electrons are intercepted by the grid bar, but the crystal may be imaged using the diffracted beam (broken lines). (b) Showing tilted illumination adjusted so that the transmitted beam is not intercepted by the grid bar, permitting observation of the chosen crystal in bright-field.

separated by large distances (typically hundreds of nanometres) and in a polycrystalline specimen it is often impossible to locate or recognize the ghosts. A useful method which can be used to find ghosts, which can then be used for the measurement of defocus, is to translate the specimen until a grid bar comes into the field of view. Ghosts displaced into the region of the grid-bar shadow are clearly visible (see Fig. 13) and the shape will usually be sufficient to identify a particular ghost with the corresponding bright-field image. A further increment of defocus shifts the ghost along the line joining it to the bright-field image, and this property can be used to confirm correct identification.

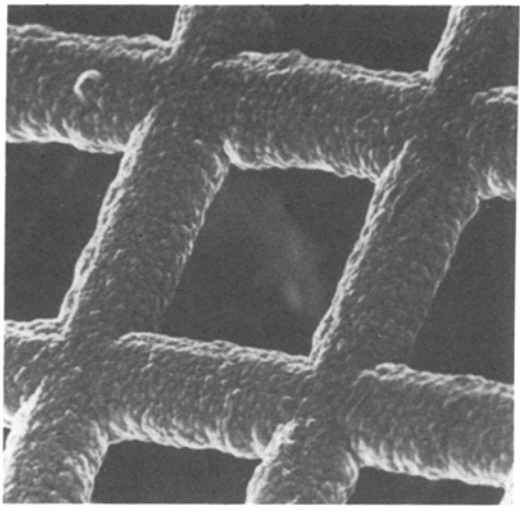

Figure 15 Scanning electron micrograph of a 300 mesh copper electron microscope grid of the kind used in the work reported here, showing the rounded profile of the grid bars.

When employing this technique we have found that a number of ghosts in the grid-bar shadow could not be positively identified, and many of these remained visible in the grid-bar shadow when the image was focused. At focus there should be no separation of the bright-field image and the ghost, and this gave a clue to the explanation of these images. Consider the cross-section of the specimen as shown in Fig. 14a. The grid bar has a somewhat rounded profile (Fig. 15) and as a consequence a small crystal in position B, just inside the geometric shadow of the grid bar, will not be seen in bright-field. A diffracted beam such as the one shown may however bypass the grid bar, and may continue forward to the image if there is no objective aperture to intercept it. Thus when the image is in focus this diffracted beam will form an image at a position corresponding to B, that is within the grid-bar shadow. We have confirmed this by tilting the electron illumination as shown in Fig. 14b so that the transmitted beam through B misses the grid bar; the bright-field image shifts, resulting in a bright-field image of the crystal at B appearing near to (but not within) the grid-bar shadow which has moved to a new position. The pair of micrographs shown in Fig. 16 clearly illustrate this, and the dark-field images in the grid-bar shadow in Fig. 16a clearly correspond to crystals which are revealed in bright-field in (Fig. 16b) after tilting the illumination.

Further confirmation of this source of ghosts

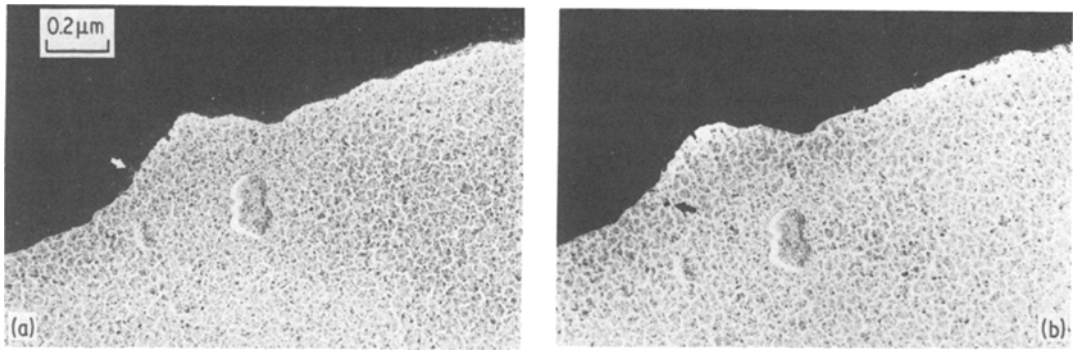

Figure 16 Single-exposure images of the area shown in Fig. 13, again taken with no objective aperture. (a) Untilted illumination; (b) illumination tilted through 0.66°. The arrows point towards a strongly diffracting crystal, imaged as a bright ghost in the grid bar shadow in (a) and appearing dark in (b). Note that these images are in focus, and there is no displacement between the crystal images in (a) and (b); it is the grid-bar shadow that has shifted.

was obtained by inverting the specimen, so that the grid bar faced the illumination source. With this arrangement far fewer ghosts were visible and, with the exception of very faint images seen only in long exposures on sensitive film, all of those which remained occupied a narrow band (< 20 nm wide) just inside the grid-bar shadow (Fig. 17). A possible explanation for these images could be that they are formed by crystals lying within the geometric shadow of the overhanging grid bar and which are illuminated either by the high-angle tail of the non-parallel portion of the incident beam, or alternatively by Fresnel diffraction from the edge of the grid bar (which will be out of focus) as in Fig. 18. If the illumination is tilted sufficiently, the change in the diffraction condition may cause ghosts to disappear or new ones to be excited. Drawn polyethylene film again provides a convenient specimen with which to illustrate this phenomenon, because of the large separation of diffracting crystals and the consequent easy identification and good contrast of their associated ghosts. In Fig. 19 several crystals are shown for which the most prominent ghost appears to move from one side of the crystal to the other on changing the illumination direction. This is because the tilt can be sufficient to lose the strong Bragg diffraction from the original reflection (**g**) while at the same time approaching the Bragg condition for the $-\mathbf{g}$ reflection. This is

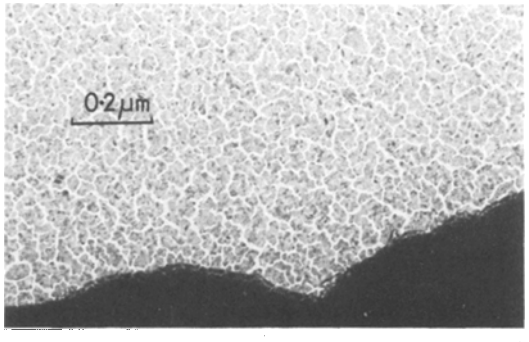

Figure 17 Polycrystalline gold film inserted into the electron microscope with the film side downwards (grid bars towards the electron illumination source) and imaged with no objective aperture inserted. Bright-field contrast continues into the grid-bar shadow for a short distance at low contrast. This contrast is easily distinguished from that of displaced (reversed-contrast) ghost images because of its appearance, and because the image coincides with the location of the crystal. Ghost images are also visible and can be made to shift deep into the grid bar shadow by defocusing, just as with images formed when the film is mounted on the upper side of the grid.

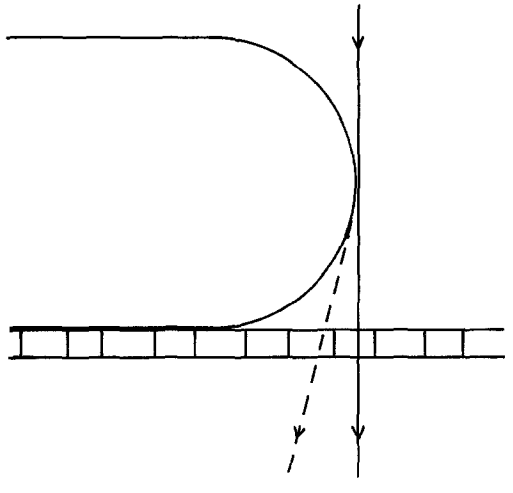

Figure 18 Schematic diagram of polycrystalline film mounted on underside of grid, showing illumination of a crystal in the grid-bar shadow resulting from diffraction at the grid-bar edge.

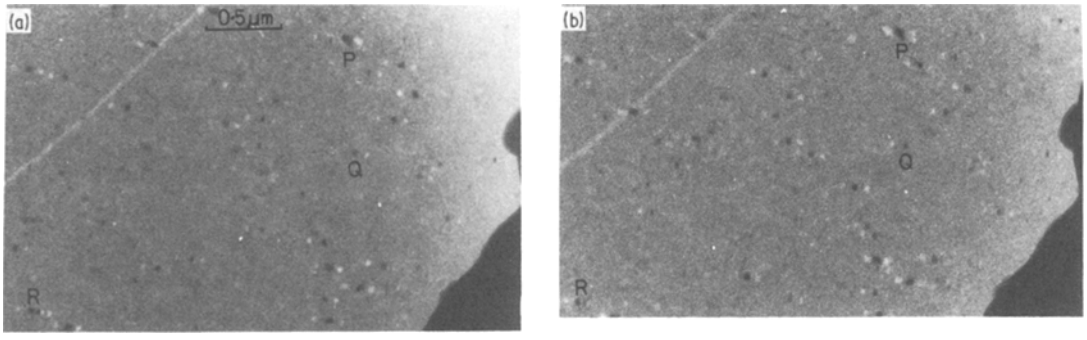

Figure 19 Defocused images of ordered polycrystalline polyethylene recorded without an objective aperture to permit observation of ghosts using (a) untilted illumination and (b) illumination tilted through 0.5°. Examples of crystals for which the more prominent ghost lies on the opposite side of the crystal in the two images are indicated by letters P, Q and R.

illustrated by the Ewald sphere construction in Fig. 20.

5.4. Estimation of crystal thickness

In Section 3.1 it was noted that the amount of misorientation from the Bragg position which can be applied to a crystal, while still retaining detectable diffraction, is inversely proportional to the crystal thickness. This effect can be exploited to give an estimate of crystal thickness if the limiting misorientation on either side of the diffracting position can be determined, and if kinematical conditions can be assumed. It is unlikely that this method could be applied to gold, for the crystals usually grow from discrete separated nuclei in an island-like manner and do not begin to become flat until the thickness reaches tens of nanometres; electron-optical kinematical conditions will then no longer apply. Techniques suitable for crystals displaying dynamical diffraction have been described elsewhere [2, 15, 16]. On the other hand, there are many reports of flat polymer crystals in the thickness range 5 to 50 nm, for which kinematical conditions should apply (say at the typical 100 keV accelerating potential) because of the low atomic numbers of the elements of which they are composed.

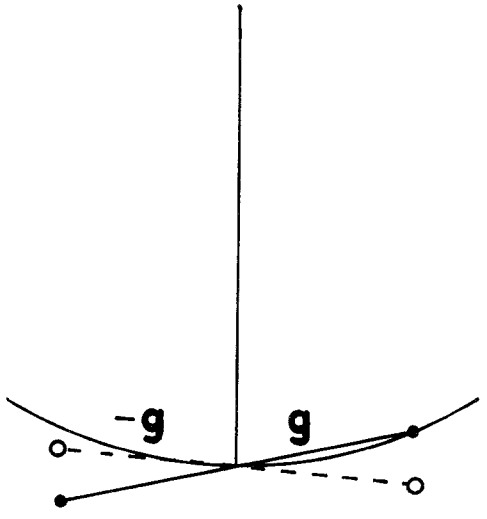

Figure 20 Ewald sphere construction showing the diffraction conditions for two crystal orientations. For one, the crystal is almost exactly Bragg-oriented for the **g** reflection (solid line); for the other, the $-\mathbf{g}$ reflection will be the stronger (broken line). (Strictly, to represent the tilted illumination conditions actually used the Ewald sphere should be rotated and the reciprocal lattice remain fixed, but this results in a more cluttered diagram).

The ideal procedure would be to choose a crystal which diffracts strongly in a chosen dark-field image and then to tilt the illumination by an ever-increasing amount, while at the same time adjusting the position of the objective aperture so that the image is always formed with the same portion of the scattering distribution. The tilt required to just cause the chosen crystal to disappear should be recorded, and tilt then applied in the opposite sense to locate the position at which diffraction just ceases on the other side of the exact Bragg orientation.

In the case of polymer crystals, their high beam-sensitivity does not permit such a procedure, which involves prolonged electron irradiation at illumination levels suitable for direct visual observation on the phosphor screen. It is common to operate a TEM at sub-visual levels while observing polymer crystals, recording images on sensitive plates or film with long exposures appropriate to the low intensities used [17]. The

information contained on the photographs is therefore not revealed until the plate or film is processed. With tilted-beam operation the tilts and the aperture positioning must be set as rapidly as possible while observing the diffraction pattern, and the usual method of low intensity with long exposure must be used for recording images. The best method appears to be to record several images, each with a different illumination tilt, and to analyse the images subsequently. The same would apply to bright-field studies. In a sequence of images taken with different tilts it should be possible to find a crystal which diffracts strongly in one position, and shows progressive reduction for tilts on either side until it becomes invisible. The total rotation between these two limits can be used to give an estimate of the limiting misorientations at which $|s| = 1/t$. The precision with which these positions can be determined depends on the interval between successive tilt settings, and this in turn will be determined by the radiation sensitivity of the specimen.

5.5. Electron-diffraction structure analysis

The use of electron diffraction for crystal structure determination is a valuable technique yet is somewhat neglected, especially in the study of polymers, though Dorset and his collaborators have made significant contributions in this area ([18–23], and citations therein to earlier work). One of the problems hampering progress is that it is difficult to obtain good data with radiation-sensitive materials. It is often required that the crystal must be oriented so that the incident beam is exactly parallel to a particular crystal axis. The necessary adjustment is made using a goniometer stage, but although it is sensible to make any coarse adjustment in this manner we recommend making the final adjustment using beam tilt, both for speed and accuracy. We concede, however, that this does not remove the major problem of recognizing the attainment of the symmetric position, and the degree of success will not be known until the plate has been processed and the intensity levels measured.

A further problem with structural analysis by electron diffraction is the influence of crystal bending on the diffracted-beam intensity levels. As mentioned in previous sections, the bending of thin crystals happens very readily; yet in electron-diffraction structure determinations it is particularly advantageous to work with very thin crystals, so as to avoid the effects of multiple scattering which are difficult to deconvolute. Consequently, bending must be expected as a frequent occurrence and the model calculations by Moss and Dorset [20–23] have confirmed the importance of taking this into account. An accurate measure of crystal bending would enhance the analysis; we suggest that after recording a diffraction pattern it might be worthwile conducting some tilt experiments on the same area, using the beam-tilt techniques described above for best accuracy, so as to attempt to estimate the local magnitude of bending.

6. Conclusions

The standard methods of operation of a conventional TEM, as described in text books and microscope manuals, relate to large single crystals which are stable in the electron beam; this permits prolonged observation and careful adjustment of the operating conditions. Such methods require considerable modification when examining radiation-sensitive samples such as polymer crystals. Polycrystalline samples with small crystallite dimensions present particular problems. Techniques for examining such samples have been discussed recently by Chacko, Adams and Thomas [9], and the interpretation of the images obtained depends on careful consideration of the diffraction conditions. In the present paper we have concentrated on examining how image contrast changes when the illuminating beam is tilted. Even small tilts can produce significant changes in contrast and, in combination with the procedures described before [9], including examination using a scanning TEM with a convergent beam, exploitation of this method should assist detailed structural analyses of polycrystalline specimens. It has been confirmed that these procedures can be used for polyethylene, which is highly susceptible to electron-beam damage.

Tilting the electron beam using the electromagnetic controls provided on most modern electron microscopes is recommended in preference to adjustment of the diffraction condition using a goniometer because of the speed, simplicity and accuracy of this method of adjustment. The inferior resolution which results from the procedure does not become limiting in many practical cases, particularly when using radiation-

sensitive specimens, because low magnification is then essential and resolution is normally determined by the recording system rather than by the electron-optical properties of the microscope [24]. It has been emphasized that tilting the illumination can be valuable for bright-field observation as well as for dark-field.

Acknowledgements

We are grateful to D. C. Yang for providing oriented polyethylene samples. Financial support from the US Air Force through contracts F33615–78–C–5175 and F33615–K–5068 is gratefully acknowledged.

References

1. P. B. HIRSCH, A. HOWIE, R. B. NICHOLSON, D. W. PASHLEY and M. J. WHELAN, "Electron Microscopy of Thin Crystals" (Butterworths, London, 1965).
2. G. THOMAS and J. M. GORINGE, "Transmission Electron Microscopy of Materials" (Wiley, New York, 1979).
3. Y. TAKAI, H. HASHIMOTO and H. ENDOH, *Acta Crystall.* **A39** (1983) 516.
4. H. HASHIMOTO, H. ENDOH, T. TANJI, A. ONO and E. WATANABE, *J. Phys. Soc. Jpn.* **42** (1977) 1073.
5. J. R. WHITE, *Thin Solid Films* **22** (1974) 23.
6. J. PETERMANN and R. M. GOHIL, *J. Mater. Sci.* **14** (1979) 2260.
7. J. PETERMANN, R. M. GOHIL and M. MASSUD, *ibid.* **17** (1982) 100.
8. D. C. YANG and E. L. THOMAS, *ibid.* **19** (1984) 2098.
9. V. P. CHACKO, W. W. ADAMS and E. L. THOMAS, *ibid.* **18** (1983) 1999.
10. E. E. LAUFER, J. T. JUBB and K. S. MILLIKEN, *J. Phys. E* **8** (1975) 671.
11. J. T. JUBB and E. E. LAUFER, *ibid.* **9** (1976) 871.
12. P. TAMBUYSER, *ibid.* **16** (1983) 483.
13. M. BORN and E. WOLF, "Principles of Optics", 6th Edn. (Pergamon, Oxford, 1980).
14. F. A. JENKINS and H. E. WHITE, "Fundamentals of Optics", 3rd Edn. (McGraw Hill, New York 1957).
15. P. M. KELLY, A. JOSTONS, R. G. BLAKE and J. G. NAPIER, *Phys. Status Solidi a* **31** (1975) 771.
16. S. M. ALLEN, *Phil. Mag.* **A43** (1981) 325.
17. J. R. WHITE, *Polymer* **16** (1975) 157.
18. D. L. DORSET and W. A. PANGBORN, *Chem. Phys. Lipids* **30** (1982) 1.
19. D. L. DORSET, *Acta Crystall.* **A36** (1980) 592.
20. B. MOSS and D. L. DORSET, *ibid.* **A38** (1982) 207.
21. *Idem, J. Polym. Sci., Polym. Phys. Ed.* **20** (1982) 1789.
22. *Idem, J. Macromol Sci., Phys.* **B22** (1983) 69.
23. D. L. DORSET and B. MOSS, *Polymer* **24** (1983) 291.
24. E. L. THOMAS and D. G. AST, *ibid.* **15** (1974) 37.

Received 16 July
and accepted 31 July 1984